IEEE Access
Multidisciplinary | Rapid Review | Open Access Journal

Received September 6, 2019, accepted October 11, 2019, date of publication October 18, 2019, date of current version October 30, 2019.

Digital Object Identifier 10.1109/ACCESS.2019.2948284

Generalized Correntropy Predictive Control for Waste Heat Recovery Systems Based on Organic Rankine Cycle

MIFENG REN[1], (Member, IEEE), MINGYUE GONG[1], MINGMING LIN[2], AND JIANHUA ZHANG[3], (Member, IEEE)

[1]College of Electrical and Power Engineering, Taiyuan University of Technology, Taiyuan 030024, China
[2]School of Automation and Electronic Engineering, Institute of Artificial Intelligence and Control, Qingdao University of Science and Technology, Qingdao 266061, China
[3]State Key Laboratory of Alternate Electrical Power System with Renewable Energy Sources, North China Electric Power University, Beijing 102206, China

Corresponding author: Mingming Lin (linmm1232008@126.com)

This work was supported in part by the Shandong Provincial Natural Science Foundation, China under Grant ZR2017LF008, in part by the Natural Science Foundation of China under Grant 61503271, Grant 61374052, Grant 61511130082, Grant 61973116, and Grant 61603136, and in part by Shanxi under Grant 201701D221112.

ABSTRACT Organic Rankine cycle (ORC) is one of the most promising technologies to recover energy from low temperature waste heat. The heat sources usually experience fluctuations in temperature and mass flow rate, which makes it difficult to obtain satisfactory control performances of ORC systems. In this paper, a single neuron adaptive multi-step predictive control scheme is developed for an ORC based waste heat recovery (WHR) system with non-Gaussian disturbances. Since the non-Gaussian disturbances existed in WHR system follow heavy-tailed distribution, generalized correntropy is adopted as the performance index to characterize the system uncertainties. The weights of the single neuron controller are updated by optimizing the performance function. The whole implementation procedures of the proposed control strategy for the WHR are presented. As a contrast, the performances of the minimum error entropy (MEE) based controller and the mean square error (MSE) based controller are also tested. The proposed control scheme is confirmed to be more effective through simulations.

INDEX TERMS ORC, waste heat recovery, generalized correntropy, single neuron adaptive multi-step predictive control, non-Gaussian.

I. INTRODUCTION

To reduce fuel consumption and achieve high energy conversion efficiency, organic Rankine cycle (ORC) based waste heat recovery (WHR) is promoted by governments around the world nowadays. Organic Rankine cycle is one of the most promising technologies for low grade heat recovery [1]. Due to its high efficiency and low maintenance, ORCs have been successfully applied in many fields, such as geothermal power plants, solar thermal power systems, desalination systems, ocean thermal conversion systems and waste heat recovery systems [2]–[8].

To obtain more efficient energy conversion, better power quality and safety, control system design for ORC based WHR is essential and important. Conventional Proportional-Integral-Derivative (PID) control is the most common control algorithm used in ORCs. In [9], the evaporating pressure control and the superheat degree control were achieved by two PI single loops. Similarly, two PI controllers with anti-windup functionality were used to keep steam pressure and temperature at desired values in [10]. To regulate superheat degree and evaporating pressure, Peralez *et al.* [11] designed a gain-scheduled PID controller and a nonlinear feedback controller based on state estimation. Although PID controller is easy to design and to be implement in practice, it is usually effective in one specific working condition.

In order to obtain satisfactory performances in wide range of working conditions, some advanced control techniques were applied into ORCs. Reference [12] examined the application of a gain scheduling controller based on

The associate editor coordinating the review of this manuscript and approving it for publication was Zhiguang Feng.

linear parameter varying (LPV) model to a WHR over the entire defined operation region. A constrained model predictive controller (MPC) was presented to control an ORC based WHR considering the system nonlinearities as well as inputs and outputs constraints [13]. In Reference [14], MPC was proposed for a WHR to track the optimal references obtained from a steady-state optimization, and an extended Kalman filter was employed for estimation of the model-plant mismatches. In light of the system nonlinearities, a switching model predictive control strategy was designed for the WHR [15]. In [16], an adaptive MPC was designed and implemented for a 11kW ORC unit to maximize power generation.

Besides nonlinearities and variable couplings, the highly fluctuating nature in the temperature and mass flow rate of waste heat, makes the control of ORCs a challenging task. To deal with stochastic disturbances from heat source, minimum variance control (MVC) strategy was presented for an ORC based WHR [17]. In [18], a multi-loop robust H_2 control scheme under partial least squares (PLS) framework was designed to resist the disturbances. The mean square error (MSE) is widely used as a cost function due to its smoothness, mathematical tractability and low computation burden. MSE works well under the assumption that the disturbances are Gaussian distributed. However, its performance may degrade considerably when the system is disturbed by non-Gaussian noises. In fact, the stochastic disturbances in WHRs are not necessarily Gaussian. Moreover, the nonlinearities in WHRs could lead to non-Gaussian randomness even if the disturbances follow a Gaussian distribution. Therefore, entropy was chosen as the indicator of system performance instead of variance or mean value of variables [19]–[22].

Minimum error entropy (MEE) based stochastic control algorithm has been applied to non-Gaussian systems [23]–[25], and the control performances are satisfactory. But when non-Gaussian disturbances follow heavy-tailed distribution, MEE will not provide effective results. In this paper, the inlet temperature and the mass flow rate of the exhaust gas are non-Gaussian disturbances in the ORC system, which follow the heavy-tailed distribution as shown in Figure 1. Thus, correntropy, a local nonlinear similarity measurement, is introduced. Due to its insensitivity to outliers, especially with a small kernel bandwidth, correntropy is a robust adaptation cost naturally. The generalized correntropy (GC), a generalization of correntropy, has better stability than correntropy. Therefore, GC criterion is adopted.

In this paper, a single neuron adaptive multi-step predictive control strategy based on generalized correntropy is proposed for an ORC based WHR disturbed by non-Gaussian noises. The paper is organized as follows: Section II introduces the ORC based WHR and describes the control tasks. In section III, the single neuron adaptive multi-step predictive controller based on generalized correntropy for the ORC is presented. Section IV demonstrates the application of the proposed controller in the ORC based WHR. Finally, some conclusions are drawn in section V.

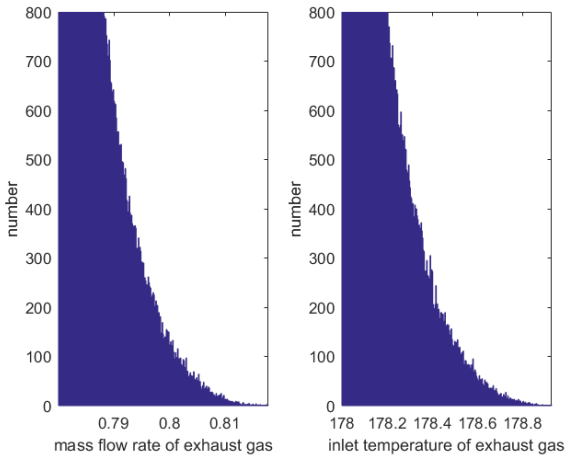

FIGURE 1. Distribution of disturbances in the WHR.

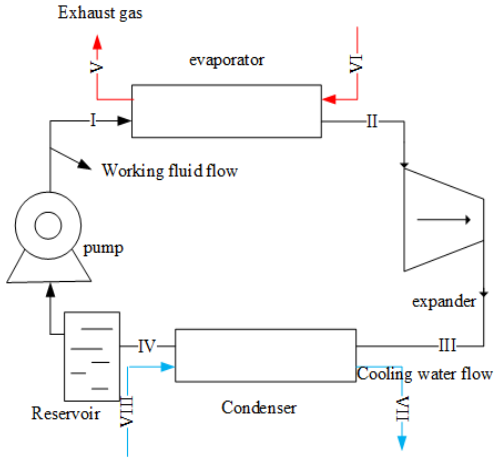

FIGURE 2. Working schematic diagram of ORC based WHR.

II. SYSTEM DESCRIPTION AND CONTROL TASKS

Figure 2 shows the considered ORC based WHR system. It mainly consists of an evaporator, an expander, a condenser, a pump and a reservoir. The detailed description of the cycle is as follows:

I-II. The organic working fluid R123 is heated into superheated vapor with certain pressure and temperature by waste gas in the evaporator.

II-III. The vapor drives the expander for power generation, and the high-pressure vapor is transformed into low-pressure vapor.

III-IV. The low-pressure vapor discharged from the expander is condensed into liquid in the condenser by cooling water.

IV-I. The condensed working fluid R123 is collected in the reservoir and pumped back to the evaporator and the cycle is finished. Then, it goes on and on.

One of the greatest challenges for controlling the WHR is how to deal with the non-Gaussian disturbances from waste heat, especially when they obey heavy-tailed distribution. The main control task considered in this paper is to ensure

TABLE 1. The definition of parameters involved in equation (1).

Parameter	MEANINGS	Unit
l_{ev}	the length of two-phase section	m
P_{ev}	the evaporating pressure	kPa
$T_{w,ev}$	the temperature of the evaporator wall	$^{\circ}C$
P_{con}	the condensing pressure	kPa
$T_{w,\text{con}}$	the temperature of the condenser wall	$^{\circ}C$
N_{exp}	the rotational speed of the expander	r/min
N_{pp}	the rotational speed of the pump	r/min
$\dot{m}_a$	the mass flow rate of the exhaust gas	kg/s
T_a	the inlet temperature of the exhaust gas	$^{\circ}C$

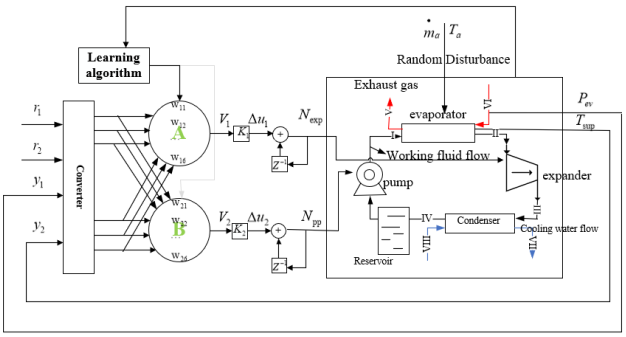

FIGURE 3. A schematic diagram of neuron adaptive control for the WHR.

WHR operates safely and efficiently in the presence of fluctuations in mass flow rate and inlet temperature of waste gas. The evaporating pressure and the superheat degree are the most important parameters in WHR, and they should be maintained in a proper range.

Therefore, the controlled variables (CVs) are the evaporating pressure and the superheat degree. The expander speed and the pump speed are chosen as the manipulated variables (MVs).

III. SINGLE NEURON STOCHASTIC PREDICTIVE CONTROL STRATEGY FOR THE WHR

In this section, the model of ORC system in [18] with non-Gaussian noises is adopted to generate data for controller design:

$$\dot{\mathbf{x}} = g(\mathbf{x}, \mathbf{u}, \mathbf{d}) \tag{1}$$

where $\mathbf{x} = \left[l_{ev}, P_{ev}, T_{w,ev}, P_{con}, T_{w,con}\right]^T$, $\mathbf{u} = \left[N_{\text{exp}}, N_{pp}\right]^T$, $\mathbf{d} = [\dot{m}_a, T_a]^T$.

The schematic diagram of neuron adaptive control system for the WHR is shown in Figure 3. In Figure 3, $[y_1,\ y_2]^T$ stands for the controlled variables, evaporating pressure P_{ev} and the superheat degree T_{sup}. $[r_1,\ r_2]^T$ represents the setpoints of P_{ev} and T_{sup} respectively. $[u_1,\ u_2]^T$ is the rotating speed of the expander N_{exp} and rotating speed of the pumpN_{pp}. T_a represents the inlet temperature of waste gas and $\dot{m}_a$ represents the mass flow rate of waste gas, and they are non-Gaussian noises. The goal of designing controller is to ensure the evaporating pressure P_{ev} and the superheat degree T_{sup} can track their setpoints r_1 and r_2 well, and the shapes of the probability density functions (PDFs) of the tracking errors become as narrow as possible. There are two control loops in the Figure 3. The evaporating pressure is controlled by the speed of the expander and the superheat degree is controlled by the speed of the pump.

A. GENERALIZED CORRENTROPY BASED PERFORMANCE INDEX

In the previous works [26], [27], the mean square error (MSE) is widely used as a cost function in controller designing when the signal is Gaussian. Since the mass flow rate and inlet temperature of waste gas are non-Gaussian and they usually follow heavy-tailed distribution, generalized correntropy is adopted to characterize the randomness of the ORC. Generalized correntropy is the local measure of similarity between any two random variables, it is nonlinear and not sensitive to the outlier.

In this paper, the generalized correntropy is given by:

$$V_{\alpha,\beta}\left(\mathbf{r},\ \mathbf{y}\right) = E\left[\mathbf{G}_{\sum_{\alpha,\beta}}\left(\mathbf{r}-\mathbf{y}\right)\right] \tag{2}$$

where $\mathbf{r} = [r_1, r_2]^T$ represents the setpoint, $\mathbf{y} = [y_1, y_2]^T$ stands for the controlled output, $E(\cdot)$ denotes the expectation operator, $\mathbf{G}_{\sum_{\alpha,\beta}}(\cdot)$ stands for the joint generalized Gaussian density (GGD) function, which is defined as:

$$\mathbf{G}_{\sum\alpha,\beta}(\cdot) = \prod_{i=1}^{2} G_{\alpha,\beta}(r_i - y_i) \tag{3}$$

where

$$\begin{aligned} G_{\alpha,\beta}\left(r_i - y_i\right) &= \frac{\alpha}{2\beta\Gamma\left(1/\alpha\right)} \exp\left(-\left|\frac{r_i - y_i}{\beta}\right|^{\alpha}\right) \\ &= \gamma_{\alpha,\beta} \exp\left(-\lambda\left|r_i - y_i\right|^{\alpha}\right) \quad (i = 1, 2) \end{aligned} \tag{4}$$

where $\alpha > 0$ is the shape parameter, $\beta > 0$ is the scale(bandwidth) parameter, with $\Gamma(\cdot)$ being the gamma function. $\lambda = 1/\beta^{\alpha}$ is the kernel parameter and $\gamma_{\alpha,\beta} = \alpha/\left(2\beta\Gamma\left(1/\alpha\right)\right)$ is the normalization constant.

In practice, the joint probability density function (PDF) of $\mathbf{r}$ and $\mathbf{y}$ are usually unknown; however, their samples $\{\mathbf{r}(s),\ \mathbf{y}(s)\}_{s=1}^{N}$ can be easily obtained, and can be used to estimate the generalized correntropy in Equation (2):

$$\hat{V}_{\alpha,\beta}(\mathbf{r}, \mathbf{y}) \approx \frac{1}{N}\sum_{s=1}^{N}\left[\prod_{i=1}^{2} G_{\alpha,\beta}\left(r_i(s) - y_i(s)\right)\right] \tag{5}$$

Since the GGD is an extension of the Gaussian density function, $V_{\alpha,\beta}\left(\mathbf{r},\ \mathbf{y}\right)$ is bounded and $0 < V_{\alpha,\beta}\left(\mathbf{r},\ \mathbf{y}\right) \leq V_{\alpha,\beta}\left(\mathbf{0}\right) = \left(\gamma_{\alpha,\beta}\right)^2$, and it reaches its maximum if and only if $\mathbf{r} = \mathbf{y}$ [26]. Therefore, the generalized correntropy loss (GC-loss) function, which is equivalent to the generalized correntropy criterion and can be expressed as follows:

$$\begin{aligned} J_{GC-loss} &= V_{\alpha,\beta}(\mathbf{0}) - \hat{V}_{\alpha,\beta}(\mathbf{r} - \mathbf{y}) \\ &= \left(\gamma_{\alpha,\beta}\right)^2 - \frac{1}{N}\sum_{s=1}^{N}\left[\prod_{i=1}^{2} G_{\alpha,\beta}\left(r_i(s) - y_i(s)\right)\right] \end{aligned} \tag{6}$$

Taking the control energy into consideration, the following predictive performance index is formulated:

$$\begin{aligned} J &= R_1 \sum_{i=1}^{P} J_{GC-loss}(\mathbf{e}_{k+i-1}) + R_2 \sum_{j=1}^{M} \mathbf{u}_{k+j-1}^T \cdot \mathbf{u}_{k+j-1} \\ &= R_1 \sum_{i=1}^{P} \left(V_{\alpha,\beta}(\mathbf{0}) - \hat{V}_{\alpha,\beta}\left(\mathbf{e}_{k+i-1}\right) \right) \\ &\quad + R_2 \sum_{j=1}^{M} \mathbf{u}_{k+j-1}^T \cdot \mathbf{u}_{k+j-1} \end{aligned} \tag{7}$$

where $\mathbf{e}_k = \mathbf{r}_k - \mathbf{y}_k$ is the system tracking error. P and M are the prediction horizon and the control horizon respectively, and $M \leq P$. The second term of Equation (7) is the constraint on system energy. R_1 and R_2 are weights that correspond to generalized correntropy and control inputs.

Remark 1: In practical situations, samples $\{\mathbf{r}(s),\ \mathbf{y}(s)\}_{s=1}^{N}$ can be obtained using the oversampling method [28], i.e. dividing the time period, from time instant k to the next time instant $k+1$, into N time periods for oversampling. This method can be sampled online, and it is more practical than the Monte Carlo method.

B. ADAPTIVE MULTI-STEP PREDICTIVE CONTROLLER BASED ON SINGLE NEURON

The single neuron adaptive multi-step predictive controller has advantages of simple structure, less calculation, fast learning and rapid adjustment. Here, a multiloop single neuron adaptive multi-step predictive control strategy for the ORC based WHR is presented as shown in Figure 3.

In Figure 3, the inputs of each single neuron are

$$\mathbf{o}_k = \begin{bmatrix} \mathbf{o}_{1k} \\ \mathbf{o}_{2k} \\ \mathbf{o}_{3k} \end{bmatrix} = \begin{bmatrix} \mathbf{e}_k \\ \mathbf{e}_k - \mathbf{e}_{k-1} \\ \mathbf{e}_k - 2\mathbf{e}_{k-1} + \mathbf{e}_{k-2} \end{bmatrix} \tag{8}$$

The controller produces the following inputs

$$\mathbf{u}_k = \mathbf{u}_{k-1} + \mathbf{K} \times \mathbf{v}_k \tag{9}$$

where

$$\mathbf{K} = diag\{K_1, K_2\} \tag{10}$$

$$\mathbf{v}_k = diag\left\{ \|\mathbf{w}_{1k}\|^{-1}, \|\mathbf{w}_{2k}\|^{-1} \right\} \times \mathbf{w}_k \times \mathbf{o}_k \tag{11}$$

$$\mathbf{w}_k = \left[\mathbf{w}_{1k}^T, \mathbf{w}_{2k}^T \right]_{2\times 6}^T = \left[w_{ij} \right]_{2\times 6} \tag{12}$$

$$\|\mathbf{w}_{ik}\| = \sum_{j=1}^{6} \left| w_{ij} \right| (i = 1, 2) \tag{13}$$

$K_i > 0$ is the proportional coefficient of the neuron, and $\mathbf{w}_{1k}$ and $\mathbf{w}_{2k}$ are the weights of the two neurons.

From Equations (9)-(13), it can be seen that in order to obtain the control inputs, we need to get the weight matrix $\mathbf{w}_k$. Here the stochastic gradient algorithm is used to update the weight matrix:

$$\mathbf{w}_{k+1} = \mathbf{w}_k - \boldsymbol{\eta} \frac{\partial J}{\partial \mathbf{w}_k} \tag{14}$$

where $\boldsymbol{\eta} = diag\{\eta_1, \eta_2\}$ $(\eta_i > 0)$ is the learning rate matrix.

$$\frac{\partial J}{\partial \mathbf{w}_k} = \frac{\partial J\left(\mathbf{e}_k\right)}{\partial \mathbf{e}_k} \times \frac{\partial \mathbf{e}_k}{\partial \mathbf{w}_k} = -\frac{1}{N} \sum_{i=1}^{N} \dot{G}_{\alpha,\beta}\left(\mathbf{e}_i\right) \frac{\partial \mathbf{e}_k}{\partial \mathbf{w}_k} \tag{15}$$

The derivative of the tracking error $\mathbf{e}_k$ with respect to the weight value $\mathbf{w}_k$ can be expressed as

$$\frac{\partial \mathbf{e}_k}{\partial \mathbf{w}_k} = \frac{\partial\left(\mathbf{r}_k - \mathbf{y}_k\right)}{\partial \mathbf{w}_k} = -\frac{\partial \mathbf{y}_k}{\partial \mathbf{u}_k} \times \frac{\partial \mathbf{u}_k}{\partial \mathbf{w}_k} \tag{16}$$

The GC-based single neuron stochastic predictive controller design procedures can be summarized into the following steps:

Step 1: Initialize the weight value $\mathbf{w}_k$ and step-size $\boldsymbol{\eta}$. Select the shape parameter α and kernel parameter λ.

Step 2: Estimate the multi-step prediction of performance indicators J according to Equations (6)-(7) by using the samplings $\{\mathbf{r}(s),\ \mathbf{y}(s)\}_{s=1}^{N}$.

Step 3: Find the optimal weight according to Equation (14)-(16).

Step 4: Calculate the control input according to Equation(9).

Step 5: Collect the process output for updating. Then repeat step 2 to 5 for the next moment, $k = k + 1$.

IV. SIMULATION RESULTS

The oversampling method is used to estimate the GC-loss ($\alpha = 10,\ \lambda = 0.1$). Sampling data must be large enough to describe the dynamic properties of the plant, so we set N to be 300. The sample period T is $1s$. The initial values of the control inputs ($u_1 = 1615r/\min, u_2 = 341r/\min$) have been determined. The learning rate η_1 and η_2 in Equation (14) have an effect on the convergence speed and training results. If the learning rate is too high, it may lead to oscillation, even non-convergence. And if the learning rate is too small, it may decelerate convergence speed and lead to a longtime training process. Therefore, the learning rate η_1 and η_2 are both set to 0.0001 after several attempts.

In this section, set point tracking test is conducted to investigate the performances of the proposed controller. As a contrast, the performances of the MEE and MSE based optimization controller are also tested. The disturbances induced by the mass flow rate and inlet temperature of exhaust gas are non-Gaussian and obey the heavy-tailed distribution as shown in Figure 1. At the beginning, the mass flow rate and the inlet temperature fluctuate in a small range and experience a step change at 700s as shown in Figure 4.

At first, the evaporating pressure and the superheat degree are kept at 1520 kPa and $11.65°C$ respectively. The set point of evaporating pressure is increased from 1520kPa to 1650kPa at 300s, while the superheat degree increased from $11.65°C$ to $19.95°C$. The results are displayed in Figure 5 and Figure 6, from which we can see that the evaporating pressure and superheat degree under GC-based controller can track set points. The proposed controller performs better with shorter settling time, smaller overshoot and smaller steady

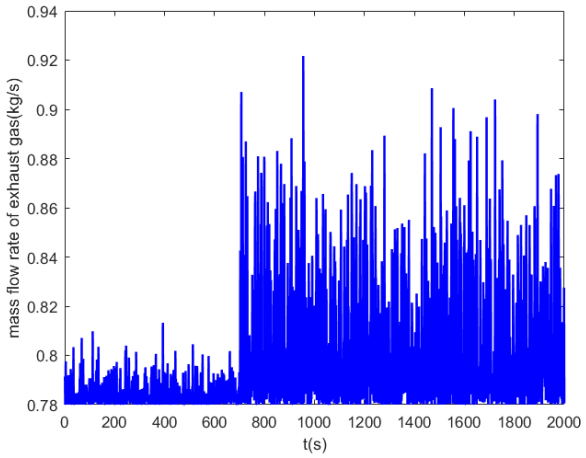

(a) Mass flow rate of the exhaust gas over time

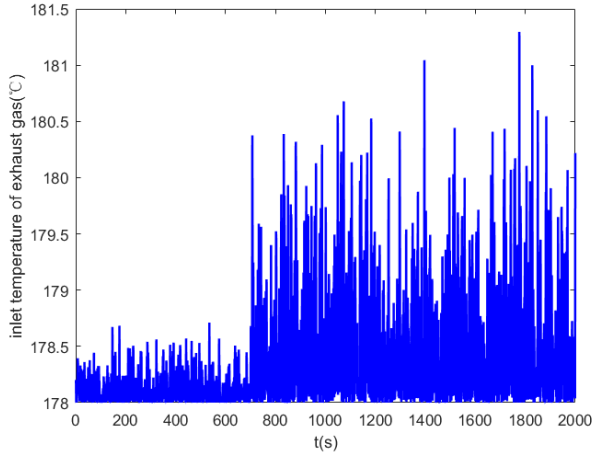

(b) Inlet temperature of the exhaust gas over time

FIGURE 4. Disturbances in the WHR.

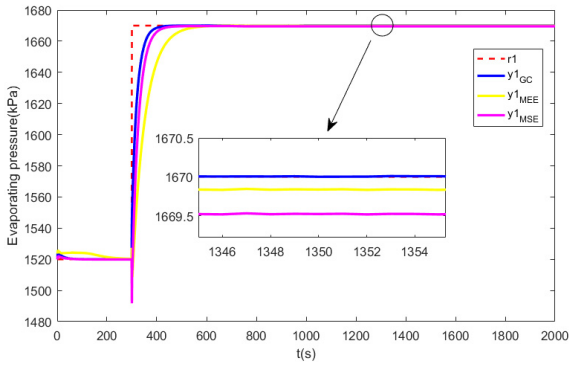

FIGURE 5. Responses of the evaporating pressure under GC-loss, MEE and MSE based control.

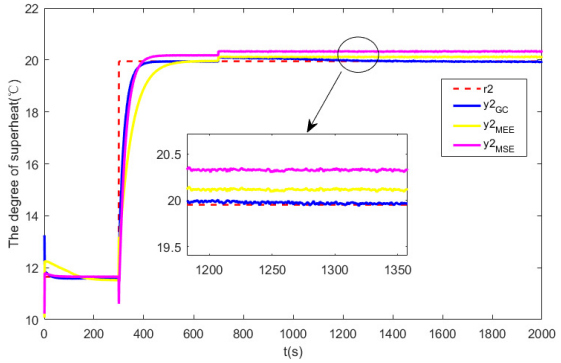

FIGURE 6. Responses of the superheat degree under GC-loss, MEE and MSE based control.

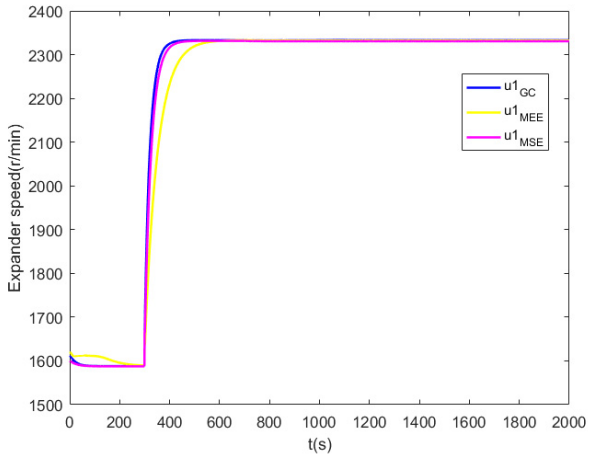

FIGURE 7. The rotating speed of the expander.

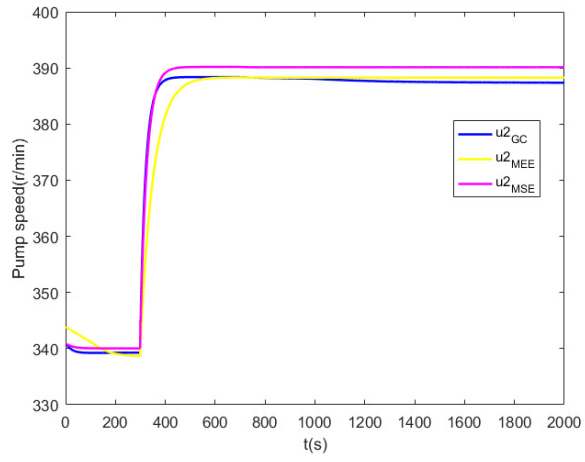

FIGURE 8. The rotating speed of the pump.

state errors. The control inputs are shown in Figure 7 and Figure 8.

The process is simulated in real-time, and Figure 9 shows the adjustment process of the weights with a duration of 2000 seconds. The entire simulation runs for about 280 seconds.

Figure 10 and Figure 11 depict the evolution of probability density function (PDF) of e_1 and e_2 at typical moments under the proposed GC-based control. The x-coordinate represents the value range of the error, and the y-coordinate represents the probability density. The higher and narrower of the PDF, the smaller the randomness is. Besides, Figure 12 and 13 illustrate the 3D PDF evolution process of tracking errors. It can be seen that the system is driven

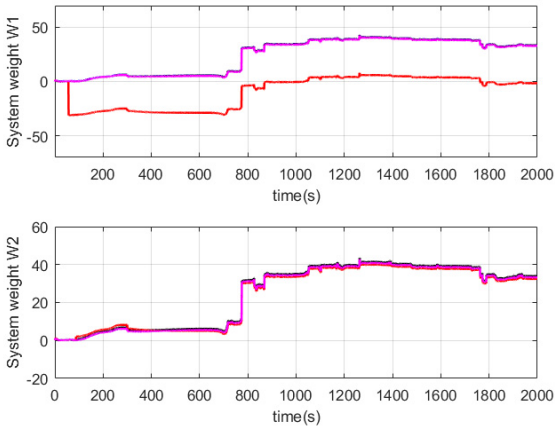

FIGURE 9. Weights of each single neuron.

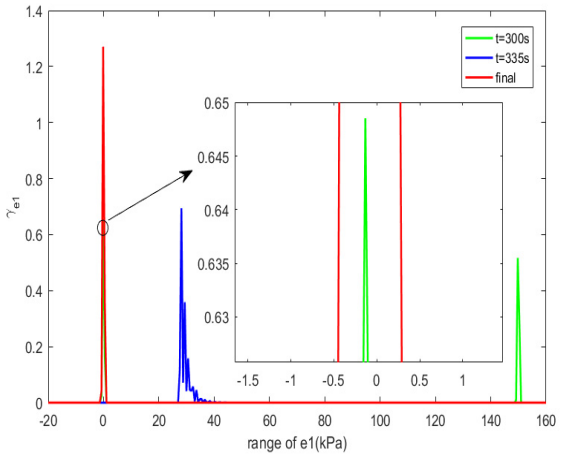

FIGURE 10. PDFs of error 1 at typical instants.

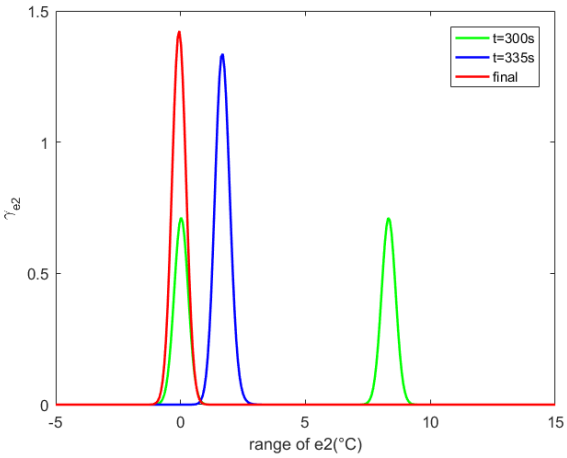

FIGURE 11. PDFs of error 2 at typical instants.

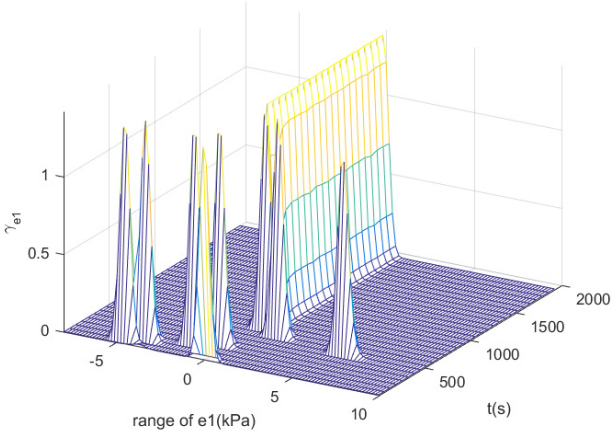

FIGURE 12. 3D PDF of tracking error 1.

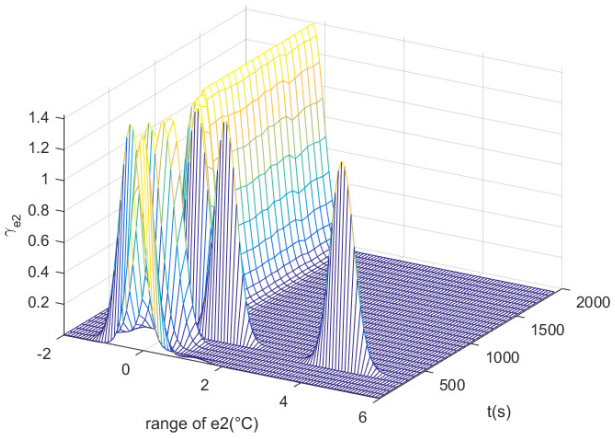

FIGURE 13. 3D PDF of tracking error 2.

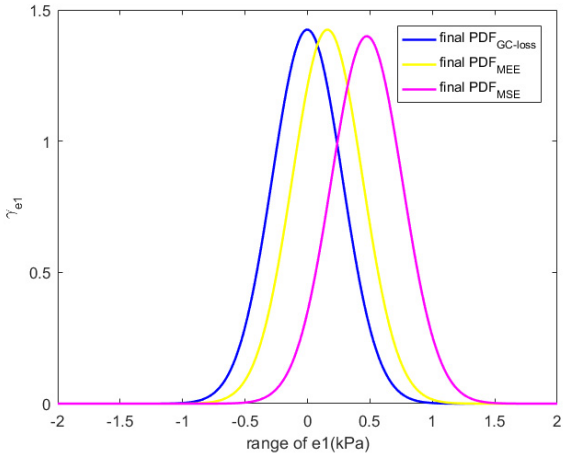

FIGURE 14. Final PDFs of e_1 under GC-loss, MEE and MSE based control.

towards a smaller randomness direction by the proposed control input. As shown in Figure 14 and 15, the PDFs of tracking errors at the last time instant are sharper and narrower under GC-based predictive control and MEE based control than that of MSE based optimization control. From the detailed views in Figure 14 and 15, it can be seen that although the randomness of the MSE optimization is small, the peak of the PDF cannot be fixed at zero, which means the track errors under the MSE control cannot be driven to zero. The mean,

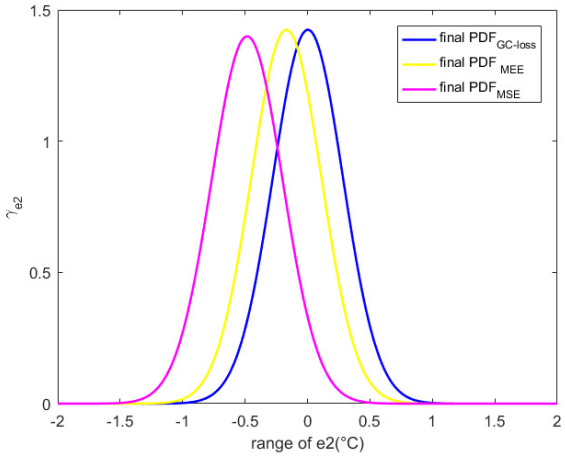

FIGURE 15. Final PDFs of e_2 under GC-loss, MEE and MSE based control.

TABLE 2. The mean, variance and entropy of tracking errors under gc-loss, mee and mse based control at 1350s.

Criterion	Errors	Mean	Variance	Entropy
GC-loss	e_1	0.043	0.0007	4.1502
	e_2	-0.0645	0.0007	
MEE	e_1	0.1635	0.0008	4.2228
	e_2	-0.1142	0.0335	
MSE	e_1	0.4793	0.0007	4.5936
	e_2	-0.426	0.037	

variance and entropy of tracking errors under GC-loss, MEE and MSE based control at 1350s is shown in Table 2.

It can be observed that the ORC based WHR achieves better performance with GC-based predictive control. The proposed controller is more advantageous in optimizing the WHR system affected by heavy-tailed disturbances.

V. CONCLUSION

In this paper, a single neuron adaptive multi-step predictive control strategy is applied to an ORC based waste heat recovery system under non-Gaussian disturbances. Instead of the entropy criterion, a generalized correntropy based performance index is adopted to optimize the controller. The simulation tests have been carried out in order to testify the control performance. The following conclusions can be summarized:

1) The GC-loss, as well as the control inputs, is constructed the performance function. The weights of each single neuron can be obtained by optimizing the performance index.
2) The evaporating pressure and the superheat degree can be kept within safe operating limits under the proposed control strategy despite the variation of set-points.
3) Randomness of the WHR is greatly decreased in the presence of non-Gaussian heavy-tailed disturbances under the proposed GC control strategy.

REFERENCES

[1] A. Mahmoudi, M. Fazli, and M. R. Morad, "A recent review of waste heat recovery by organic Rankine cycle," *Appl. Therm. Eng.*, vol. 143, pp. 660–675, Oct. 2018. doi: 10.1016/j.applthermaleng.2018.07.136.
[2] T. Li, X. Hu, J. Wang, X. Kong, J. Liu, and J. Zhu, "Performance improvement of two-stage serial organic Rankine cycle (TSORC) driven by dual-level heat sources of geothermal energy coupled with solar energy," *Geothermics*, vol. 76, pp. 261–270, Nov. 2018. doi: 10.1016/j.geothermics.2018.07.010.
[3] X. Wang, E. K. Levy, C. Pan, C. E. Romero, A. Banerjee, C. Rubio-Maya, and L. Pan, "Working fluid selection for organic Rankine cycle power generation using hot produced supercritical CO_2 from a geothermal reservoir," *Appl. Therm. Eng.*, vol. 149, pp. 1287–1304, Feb. 2019. doi: 10.1016/j.applthermaleng.2018.12.112.
[4] R. Loni, E. A. Asli-Ardeh, B. Ghobadian, G. Najafi, and E. Bellos, "Effects of size and volume fraction of alumina nanoparticles on the performance of a solar organic rankine cycle," *Energy Convers. Manage.*, vol. 182, pp. 398–411, Feb. 2019. doi: 10.1016/j.enconman.2018.12.079.
[5] P. Morrone, A. Algieri, and T. Castiglione, "Hybridisation of biomass and concentrated solar power systems in transcritical organic rankine cycles: A micro combined heat and power application," *Energy Convers. Manage.*, vol. 180, pp. 757–768, Jan. 2019. doi: 10.1016/j.enconman.2018.11.029.
[6] W. F. He, C. Ji, D. Han, Y. K. Wu, L. Huang, and X. K. Zhang, "Performance analysis of the mechanical vapor compression desalination system driven by an organic Rankine cycle," *Energy*, vol. 141, pp. 1177–1186, Dec. 2017. doi: 10.1016/j.energy.2017.10.014.
[7] M. Wang, R. Jing, H. Zhang, C. Meng, N. Li, and Y. Zhao, "An innovative Organic Rankine Cycle (ORC) based ocean thermal energy conversion (OTEC) system with performance simulation and multi-objective optimization," *Appl. Therm. Eng.*, vol. 145, pp. 743–754, Dec. 2018. doi: 10.1016/j.applthermaleng.2018.09.075.
[8] B.-S. Park, M. Usman, M. Imran, and A. Pesyridis, "Review of organic rankine cycle experimental data trends," *Energy Convers. Manage.*, vol. 173, pp. 679–691, Oct. 2018. doi: 10.1016/j.enconman.2018.07.097.
[9] S. Quoilin, R. Aumann, A. Grill, A. Schuster, V. Lemort, and H. Spliethoff, "Dynamic modeling and optimal control strategy of waste heat recovery organic Rankine cycles," *Appl. Energy*, vol. 88, no. 6, pp. 2183–2190, 2011. doi: 10.1016/j.apenergy.2011.01.015.
[10] T. A. Horst, H.-S. Rottengruber, M. Seifert, and J. Ringler, "Dynamic heat exchanger model for performance prediction and control system design of automotive waste heat recovery systems," *Appl. Energy*, vol. 105, pp. 293–303, May 2013. doi: 10.1016/j.apenergy.2012.12.060.
[11] J. Peralez, M. Nadri, P. Dufour, P. Tona, and A. Sciarretta, "Control design for an automotive turbine Rankine cycle system based on nonlinear state estimation," in *Proc. 53rd IEEE Conf. Decis. Control*, Dec. 2014, pp. 3316–3321. doi: 10.1109/CDC.2014.7039902.
[12] J. Zhang, M. Lin, F. Fang, J. Xu, and K. Li, "Gain scheduling control of waste heat energy conversion systems based on an LPV (linear parameter varying) model," *Energy*, vol. 107, pp. 773–783, Jul. 2016. doi: 10.1016/j.energy.2016.04.064.
[13] J. Zhang, Y. Zhou, R. Wang, J. Xu, and F. Fang, "Modeling and constrained multivariable predictive control for ORC (Organic Rankine Cycle) based waste heat energy conversion systems," *Energy*, vol. 66, pp. 128–138, Mar. 2014. doi: 10.1016/j.energy.2014.01.068.
[14] E. Feru, F. Willems, B. de Jager, and M. Steinbuch, "Model predictive control of a waste heat recovery system for automotive diesel engines," in *18th Int. Conf. Syst. Theory, Control Comput. (ICSTCC)*, Oct. 2014, pp. 658–663. doi: 10.1109/ICSTCC.2014.6982492.
[15] E. Feru, F. Willems, B. de Jager, and M. Steinbuch, "Modeling and control of a parallel waste heat recovery system for euro-VI heavy-duty diesel engines," *Energies*, vol. 7, no. 10, pp. 6571–6592, 2014. doi: 10.3390/en7106571.
[16] A. Hernandez, A. Desideri, S. Gusev, C. M. Ionescu, M. Van Den Broek, S. Quoilin, V. Lemort, and R. De Keyser, "Design and experimental validation of an adaptive control law to maximize the power generation of a small-scale waste heat recovery system," *Appl. Energy*, vol. 203, pp. 549–559, Oct. 2017. doi: 10.1016/j.apenergy.2017.06.069.
[17] G. Hou, S. Bi, M. Lin, J. Zhang, and J. Xu, "Minimum variance control of organic Rankine cycle based waste heat recovery," *Energy Convers. Manage.*, vol. 86, pp. 576–586, Oct. 2014. doi: 10.1016/j.enconman.2014.06.004.
[18] J. Zhang, M. Lin, J. Chen, J. Xu, and K. Li, "PLS-based multi-loop robust H2 control for improvement of operating efficiency of waste heat energy conversion systems with organic Rankine cycle," *Energy*, vol. 123, pp. 460–472, Mar. 2017. doi: 10.1016/j.energy.2017.01.131.

[19] H. Wang, "Minimum entropy control of non-Gaussian dynamic stochastic systems," *IEEE Trans. Autom. Control*, vol. 47, no. 2, pp. 398–403, Feb. 2002. doi: 10.1109/9.983388.
[20] J. Zhang, M. Ren, and H. Wang, "Minimum entropy control for non-linear and non-Gaussian two-input and two-output dynamic stochastic systems," *IET Control Theory Appl.*, vol. 6, no. 15, pp. 2434–2441, Oct. 2012. doi: 10.1049/iet-cta.2011.0791.
[21] M. Ren, J. Zhang, and H. Wang, "Minimized tracking error randomness control for nonlinear multivariate and non-Gaussian systems using the generalized density evolution equation," *IEEE Trans. Autom. Control*, vol. 59, no. 9, pp. 2486–2490, Sep. 2014. doi: 10.1109/TAC.2014.2305932.
[22] M. Ren, J. Zhang, M. Jiang, M. Yu, and J. Xu, "Minimum (h,ϕ)—Entropy control for non-Gaussian stochastic networked control systems and its application to a networked DC motor control system," *IEEE Trans. Control Syst. Technol.*, vol. 23, no. 1, pp. 406–411, Jan. 2015. doi: 10.1109/TCST.2014.2324978.
[23] J. Zhang, M. Ren, and H. Yue, "Constrained entropy-based temperature control of waste heat systems," in *Proc. 12th World Congr. Intell. Control Automat. (WCICA)*, Jun. 2016, pp. 1992–1998. doi: 10.1109/WCICA.2016.7578809.
[24] J. Zhang, F. Zhang, M. Ren, G. Hou, and F. Fang, "Cascade control of superheated steam temperature with neuro-PID controller," *ISA Trans.*, vol. 51, no. 6, pp. 778–785, 2012. doi: 10.1016/j.isatra.2012.06.008.
[25] F. Yang, H. Cho, H. Zhang, J. Zhang, and Y. Wu, "Artificial neural network (ANN) based prediction and optimization of an organic Rankine cycle (ORC) for diesel engine waste heat recovery," *Energy Convers. Manage.*, vol. 164, pp. 15–26, May 2018. doi: 10.1016/j.enconman.2018.02.062.
[26] B. Chen, L. Xing, H. Zhao, N. Zheng, and J. C. Príncipe, "Generalized correntropy for robust adaptive filtering," *IEEE Trans. Signal Process.*, vol. 64, no. 13, pp. 3376–3387, Jul. 2016. doi: 10.1109/TSP.2016.2539127.
[27] B. Chen, Y. Zhu, J. Hu, and J. C. Principe, *System Parameter Identification: Information Criteria and Algorithms*. Amsterdam, The Netherlands: Elsevier, 2013. doi: 10.1016/C2012-0-01233-1.
[28] X. Xu, Y. Zhao, M. Ren, L. Cheng, and M. Gong, "SIP-based single neuron stochastic predictive control for non-Gaussian networked control systems with uncertain metrology delays," *Entropy*, vol. 20, no. 7, p. 494, 2018.

MIFENG REN was born in Pingshan, China, in 1985. She received the M.S. degree in applied mathematics from the Hebei University of Science and Technology, Shijiazhuang, China, in 2011, and the Ph.D. degree in control theory and control engineering from North China Electric Power University, Beijing, China, in 2014. She is currently an Associate Professor with the School of Electrical and Power Engineering, Taiyuan University of Technology, Taiyuan, China. Her research interests include stochastic distribution control, control performance assessment, and fault diagnosis.

MINGYUE GONG was born in Handan, China, in 1995. She is currently pursuing the M.S. degree with the School of Electrical and Power Engineering, Taiyuan University of Technology, Taiyuan, China. Her research interest includes stochastic distribution control.

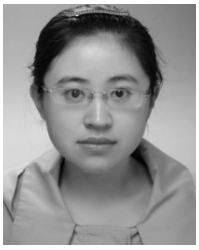

MINGMING LIN received the bachelor's degree in automation and the Ph.D. degree in control theory and control engineering from North China Electric Power University, Beijing, China, in 2010 and 2016, respectively. She is currently a Lecturer with the School of Automation and Electronic Engineering, Qingdao University of Science and Technology, Qingdao, China. Her research interests include system modeling, advanced process control, and nonlinear system control.

JIANHUA ZHANG received the Ph.D. degree in mechanical engineering from the Beijing University of Aeronautics and Astronautics, Beijing, China, in 1996. She is currently a Professor with the School of Control and Computer Engineering, North China Electric Power University, Beijing. Her research interests include integrated energy system, stochastic control, networked control systems, fault diagnosis, and process control.